We are IntechOpen, the world's leading publisher of Open Access books Built by scientists, for scientists

4,800
Open access books available

122,000
International authors and editors

135M
Downloads

Our authors are among the

154
Countries delivered to

TOP 1%
most cited scientists

12.2%
Contributors from top 500 universities

WEB OF SCIENCE™

Selection of our books indexed in the Book Citation Index in Web of Science™ Core Collection (BKCI)

Interested in publishing with us?
Contact book.department@intechopen.com

Numbers displayed above are based on latest data collected.
For more information visit www.intechopen.com

1

3D Face Recognition in a Ambient Intelligence Environment Scenario

Andrea F. Abate, Stefano Ricciardi and Gabriele Sabatino
Dip. di Matematica e Informatica - Università degli Studi di Salerno
Italy

1. Introduction

Information and Communication Technologies are increasingly entering in all aspects of our life and in all sectors, opening a world of unprecedented scenarios where people interact with electronic devices embedded in environments that are sensitive and responsive to the presence of users. Indeed, since the first examples of "intelligent" buildings featuring computer aided security and fire safety systems, the request for more sophisticated services, provided according to each user's specific needs has characterized the new tendencies within domotic research. The result of the evolution of the original concept of home automation is known as Ambient Intelligence (Aarts & Marzano, 2003), referring to an environment viewed as a "community" of smart objects powered by computational capability and high user-friendliness, capable of recognizing and responding to the presence of different individuals in a seamless, not-intrusive and often invisible way. As adaptivity here is the key for providing customized services, the role of person sensing and recognition become of fundamental importance.

This scenario offers the opportunity to exploit the potential of face as a not intrusive biometric identifier to not just regulate access to the controlled environment but to adapt the provided services to the preferences of the recognized user. Biometric recognition (Maltoni et al., 2003) refers to the use of distinctive physiological (e.g., fingerprints, face, retina, iris) and behavioural (e.g., gait, signature) characteristics, called biometric identifiers, for automatically recognizing individuals. Because biometric identifiers cannot be easily misplaced, forged, or shared, they are considered more reliable for person recognition than traditional token or knowledge-based methods. Others typical objectives of biometric recognition are user convenience (e.g., service access without a Personal Identification Number), better security (e.g., difficult to forge access). All these reasons make biometrics very suited for Ambient Intelligence applications, and this is specially true for a biometric identifier such as face which is one of the most common methods of recognition that humans use in their visual interactions, and allows to recognize the user in a not intrusive way without any physical contact with the sensor.

A generic biometric system could operate either in verification or identification modality, better known as one-to-one and one-to-many recognition (Perronnin & Dugelay, 2003). In the proposed Ambient Intelligence application we are interested in one-to-one recognition,

Source: Face Recognition, Edited by: Kresimir Delac and Mislav Grgic, ISBN 978-3-902613-03-5, pp.558, I-Tech, Vienna, Austria, June 2007

as we want recognize authorized users accessing the controlled environment or requesting a specific service.
We present a face recognition system based on 3D features to verify the identity of subjects accessing the controlled Ambient Intelligence Environment and to customize all the services accordingly. In other terms to add a social dimension to man-machine communication and thus may help to make such environments more attractive to the human user. The proposed approach relies on stereoscopic face acquisition and 3D mesh reconstruction to avoid highly expensive and not automated 3D scanning, typically not suited for real time applications. For each subject enrolled, a bidimensional feature descriptor is extracted from its 3D mesh and compared to the previously stored correspondent template. This descriptor is a normal map, namely a color image in which RGB components represent the normals to the face geometry. A weighting mask, automatically generated for each authorized person, improves recognition robustness to a wide range of facial expression.
This chapter is organized as follows. In section 2 related works are presented and the proposed method is introduced. In section 3 the proposed face recognition method is presented in detail. In section 4 the Ambient Intelligence framework is briefly discussed and experimental results are shown and commented. The paper concludes in section 5 showing directions for future research and conclusions.

2. Related Works

In their survey on state of the art in 3D and multi-modal face recognition, Bowyer et al. (Bowyer et al., 2004) describe the most recent results and research trends, showing that "the variety and sophistication of algorithmic approaches explored is expanding". The main challenges in this field result to be the improvement of recognition accuracy, a greater robustness to facial expressions, and, more recently, the efficiency of algorithms. Many methods are based on Principal Component Analysis (PCA), such is the case of Hester et al. (Hester et al., 2003) which tested the potential and the limits of PCA varying the number of eigenvectors and the size of range images. Pan et al. (Pan et al., 2005) apply PCA to a novel mapping of the 3D data to a range, or depth, image, while Xu et al. (Xu et al., 2004) aim to divide face in sub-regions using nose as the anchor, PCA to reduce feature space dimensionality and minimum distance for matching. Another major research trend is based on Iterative Closest Point (ICP) algorithm, which has been exploited in many variations for 3D shape aligning, matching or both. The first example of this kind of approach to face recognition has been presented from Medioni and Waupotitsch (Medioni & Waupotitsch, 2003), then Lu and Jain (Lu & Jain, 2005) developed an extended version aimed to cope with expressive variations, whereas Chang et al. (Chang et al., 2005) proposed to apply ICP not to the whole face but to a set of selected subregions instead.
As a real face is fully described by its 3D shape and its texture, it is reasonable to use both kind of data (geometry and color or intensity) to improve recognition reliability: this is the idea behind Multi-Modal or (3D+2D) face recognition. The work by Tsalakanidou et al. (Tsalakanidou et al., 2003) is based on PCA to compare both probe's range image and intensity/color image to the gallery, Papatheodorou and Rueckert (Papatheodorou & Rueckert, 2004) presented a 4D registration method based on Iterative Closest Point (ICP), augmented with texture data. Bronstein et al. (Bronstein et al., 2003) propose a multi-modal 3D + 2D recognition using eigen decomposition of flattened textures and canonical images. Other authors combine 3D and 2D similarity scores obtained comparing 3D and 2D profiles

(Beumier & Acheroy, 2000), or extract a feature vector combining Gabor filter responses in 2D and point signatures in 3D (Wang et al., 2003).

3. Description of Facial Recognition System

The basic idea behind proposed system is to represent user's facial surface by a digital signature called normal map. A normal map is an RGB color image providing a 2D representation of the 3D facial surface, in which each normal to each polygon of a given mesh is represented by a RGB color pixel. To this aim, we project the 3D geometry onto 2D space through spherical mapping. The result is a bidimensional representation of original face geometry which retains spatial relationships between facial features. Color info coming from face texture are used to mask eventual beard covered regions according to their relevance, resulting in a 8 bit greyscale filter mask (Flesh Mask). Then, a variety of facial expressions are generated from the neutral pose through a rig-based animation technique, and corresponding normal maps are used to compute a further 8 bit greyscale mask (Expression Weighting Mask) aimed to cope with expression variations. At this time the two greyscale masks are multiplied and the resulting map is used to augment with extra 8 bit per pixel the normal map, resulting in a 32 bit RGBA bitmap (Augmented Normal Map).
The whole process (see Figure 1) is discussed in depth in the following subsections 3.1 to 3.4..

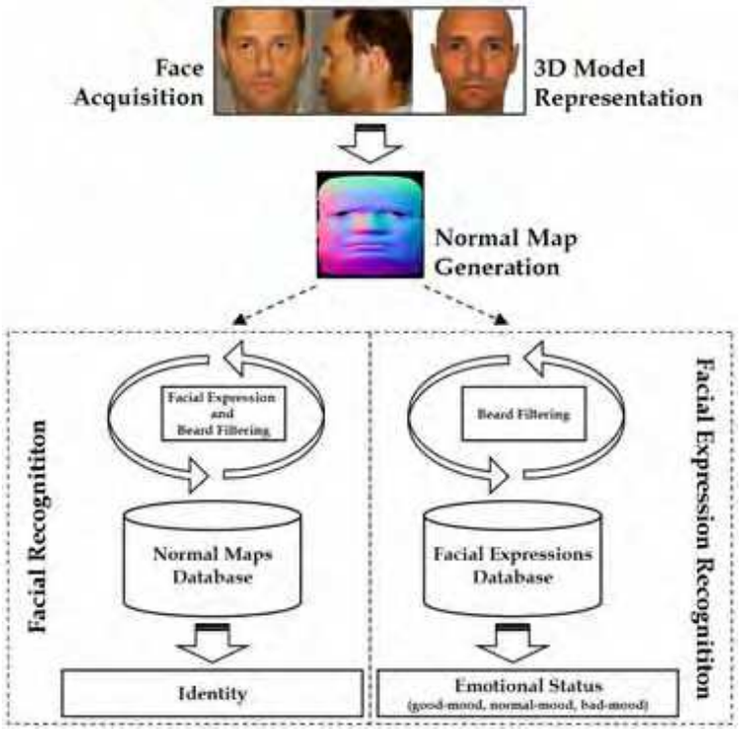

Figure 1. Facial and Facial Expression Recognition workflow

3.1 Face Capturing

As the proposed method works on 3D polygonal meshes we firstly need to acquire actual faces and to represent them as polygonal surfaces. The Ambient Intelligence context, in which we are implementing face recognition, requires fast user enrollment to avoid annoying waiting time. Usually, most 3D face recognition methods work on a range image of the face, captured with laser or structured light scanner. This kind of devices offer high resolution in the captured data, but they are too slow for a real time face acquisition. Face unwanted motion during capturing could be another issue, while laser scanning could not be harmless to the eyes.

For all this reasons we opted for a 3D mesh reconstruction from stereoscopic images, based on (Enciso et al., 1999) as it requires a simple equipment more likely to be adopted in a real application: a couple of digital cameras shooting at high shutter speed from two slightly different angles with strobe lighting. Though the resulting face shape accuracy is inferior compared to real 3D scanning it proved to be sufficient for recognition yet much faster, with a total time required for mesh reconstruction of about 0.5 sec. on a P4/3.4 Ghz based PC, offering additional advantages, such as precise mesh alignment in 3D space thanks to the warp based approach, facial texture generation from the two captured orthogonal views and its automatic mapping onto the reconstructed face geometry.

3.2 Building a Normal Map

As the 3D polygonal mesh resulting from the reconstruction process is an approximation of the actual face shape, polygon normals describe local curvature of captured face which could be view as its signature. As shown in Figure 2, we intend to represent these normals by a color image transferring face's 3D features in a 2D space. We also want to preserve the spatial relationships between facial features, so we project vertices' 3D coordinates onto a 2D space using a spherical projection. We can now store normals of mesh M in a bidimensional array N using mapping coordinates, by this way each pixel represents a normal as RGB values. We refer the resulting array as the Normal Map N of mesh M and this is the signature we intend to use for the identity verification.

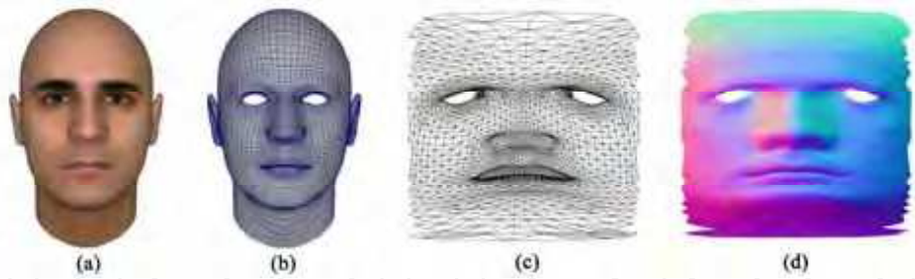

Figure 2. (a) 3d mesh model, (b) wireframe model, (c) projection in 2D spatial coordinates, (d) normal map

3.3 Normal Map Comparison

To compare the normal map N_A from input subject to another normal map N_B previously stored in the reference database, we compute through:

$$\theta = \arccos\left(r_{N_A} \cdot r_{N_B} + g_{N_A} \cdot g_{N_B} + b_{N_A} \cdot b_{N_B}\right) \tag{1}$$

the angle included between each pairs of normals represented by colors of pixels with corresponding mapping coordinates, and store it in a new Difference Map D with components *r*, *g* and *b* opportunely normalized from spatia l domain to color domain, so $0 \le r_{N_A}, g_{N_A}, b_{N_A} \le 1$ and $0 \le r_{N_B}, g_{N_B}, b_{N_B} \le 1$. The value θ, with $0 \le \theta < \pi$, is the angular difference between the pixels with coordinates (x_{N_A}, y_{N_A}) in N_A and (x_{N_B}, y_{N_B}) in N_B and it is stored in D as a gray-scale color. At this point, the histogram H is analyzed to estimate the similarity score between N_A and N_B. On the X axis we represent the resulting angles between each pair of comparisons (sorted from 0° degree to 180° degree), while on the Y axis we represent the total number of differences found. The curvature of H represents the angular distance distribution between mesh MA and MB, thus two similar faces featuring very high values on small angles, whereas two unlike faces have more distributed differences (see Figure 3). We define a similarity score through a weighted sum between H and a Gaussian function G, as in:

$$similarity\_score = \sum_{x=0}^{k} \left(H(x) \cdot \frac{1}{\sigma\sqrt{2\pi}} e^{-\frac{x^2}{2\sigma^2}} \right) \tag{2}$$

where with the variation of σ and k is possible to change recognition sensibility. To reduce the effects of residual face misalignment during acquisition and sampling phases, we calculate the angle θ using a k × k (usually 3 × 3 or 5 × 5) matrix of neighbour pixels.

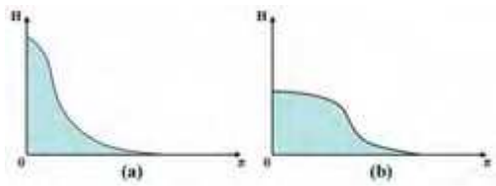

Figure 3. Example of histogram H to represent the angular distances. (a) shows a typical histogram between two similar Normal Maps, while (b) between two different Normal Maps

3.4 Addressing Beard and Facial Expressions via 8 bit Alpha Channel

The presence of beard with variable length covering a portion of the face surface in a subject previously enrolled without it (or vice-versa), could lead to a measurable difference in the overall or local 3D shape of the face mesh (see Figure 4). In this case the recognition accuracy could be affected resulting, for instance, in a higher False Rejection Rate FRR. To improve the robustness to this kind of variable facial features we rely on color data from the captured face texture to mask the non-skin region, eventually disregarding them during the comparison.

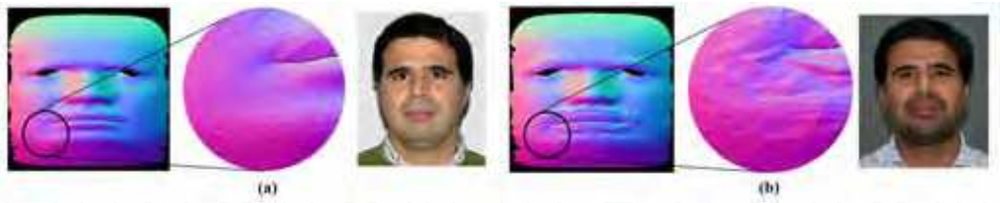

Figure 4. Normal maps of the same subject enrolled in two different sessions with and without beard

We exploit flesh hue characterization in the HSB color space to discriminate between skin and beard/moustaches/eyebrows. Indeed, the hue component of each given texel is much less affected from lighting conditions during capturing then its corresponding RGB value. Nevertheless there could be a wide range of hue values within each skin region due to factors like facial morphology, skin conditions and pathologies, race, etc., so we need to define this range on a case by case basis to obtain a valid mask. To this aim we use a set of specific hue sampling spots located over the face texture at absolute coordinates, selected to be representative of flesh's full tonal range and possibly distant enough from eyes, lips and typical beard and hair covered regions.

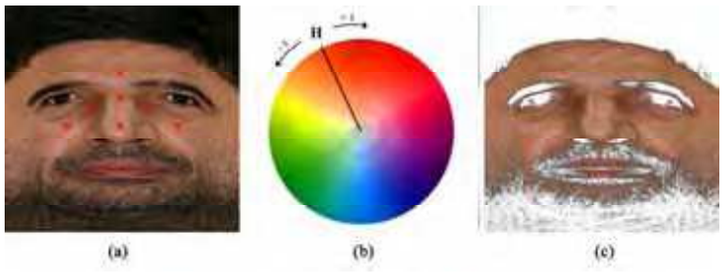

Figure 5. Flesh Hue sampling points (a), Flesh Hue Range (b) non-skin regions in white (c)

This is possible because each face mesh and its texture are centered and normalized during the image based reconstruction process (i.e. the face's median axis is always centered on the origin of 3D space with horizontal mapping coordinates equal to 0.5), otherwise normal map comparison would not be possible. We could use a 2D or 3D technique to locate main facial features (eye, nose and lips) and to position the sampling spots relative to this features, but even these approaches are not safe under all conditions. For each sampling spot we sample not just that texel but a 5 x 5 matrix of neighbour texels, averaging them to minimize the effect of local image noise. As any sampling spot could casually pick wrong values due to local skin color anomalies such as moles, scars or even for improper positioning, we calculate the median of all resulting hue values from all sampling spots, resulting in a main Flesh Hue Value *FHV* which is the center of the valid flesh hue range. We therefore consider belonging to skin region all the texels whose hue value is within the range: $-t \leq FHV \leq t$, where t is a hue tolerance which we experimentally found could be set below 10° (see Figure 5-b). After the skin region has been selected, it is filled with pure white while the remaining pixels are converted to a greyscale value depending on their distance from the selected flesh hue range (the more the distance the darker the value).

To improve the facial recognition system and to address facial expressions we opt to the use of expression weighting mask, a subject specific pre-calculated mask aimed to assign different relevance to different face regions. This mask, which shares the same size of normal map and difference map, contains for each pixel an 8 bit weight encoding the local rigidity of the face surface based on the analysis of a pre-built set of facial expressions of the same subject. Indeed, for each subject enrolled, each of expression variations (see Figure 6) is compared to the neutral face resulting in difference maps.

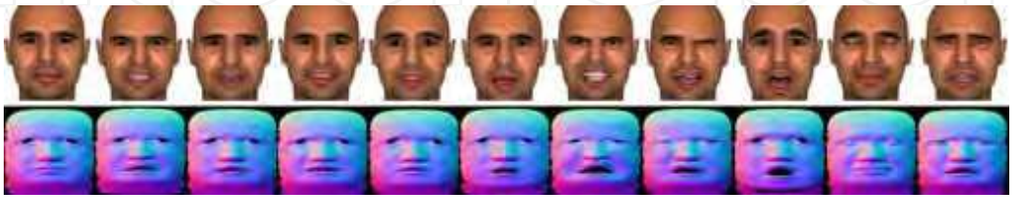

Figure 6. An example of normal maps of the same subject featuring a neutral pose (leftmost face) and different facial expressions

The average of this set of difference maps specific to the same individual represent its expression weighting mask. More precisely, given a generic face with its normal map N_0 (neutral face) and the set of normal maps N_1, N_2, …, N_n (the expression variations), we first calculate the set of difference map D_1, D_2, …, D_n resulting from {N_0 - N_1, N_0 - N_2, …, N_0 – N_n}. The average of set {D_1, D_2, …, D_n} is the expression weighting mask which is multiplied by the difference map in each comparison between two faces.

We generate the expression variations through a parametric rig based deformation system previously applied to a prototype face mesh, morphed to fit the reconstructed face mesh (Enciso et al., 1999). This fitting is achieved via a landmark-based volume morphing where the transformation and deformation of the prototype mesh is guided by the interpolation of a set of landmark points with a radial basis function. To improve the accuracy of this rough mesh fitting we need a surface optimization obtained minimizing a cost function based on the Euclidean distance between vertices.

So we can augment each 24 bit normal map with the product of Flesh Mask and Expression Weighting Mask normalized to 8 bit (see Figure 7). The resulting 32 bit per pixel RGBA bitmap can be conveniently managed via various image formats like the Portable Network Graphics format (PNG) which is typically used to store for each pixel 24 bit of colour and 8 bit of alpha channel (transparency). When comparing any two faces, the difference map is computed on the first 24 bit of color info (normals) and multiplied to the alpha channel (filtering mask).

4. Testing Face Recognition System into an Ambient Intelligence Framework

Ambient Intelligence (AmI) worlds offer exciting potential for rich interactive experiences.

The metaphor of AmI envisages the future as intelligent environments where humans are surrounded by smart devices that makes the ambient itself perceptive to humans' needs or wishes. The Ambient Intelligence Environment can be defined as the set of actuators and sensors composing the system together with the domotic interconnection protocol. People interact with electronic devices embedded in environments that are sensitive and responsive to the presence of users. This objective is achievable if the environment is capable to learn,

build and manipulate user profiles considering from a side the need to clearly identify the human attitude; in other terms, on the basis of physical and emotional user status captured from a set of biometric features.

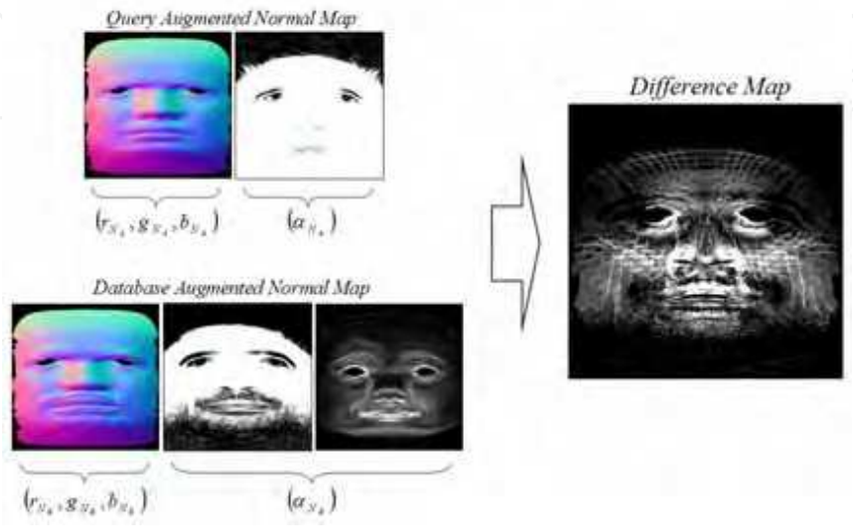

Figure 7. Comparison of two Normal Maps using Flesh Mask and the resulting Difference Map (c)

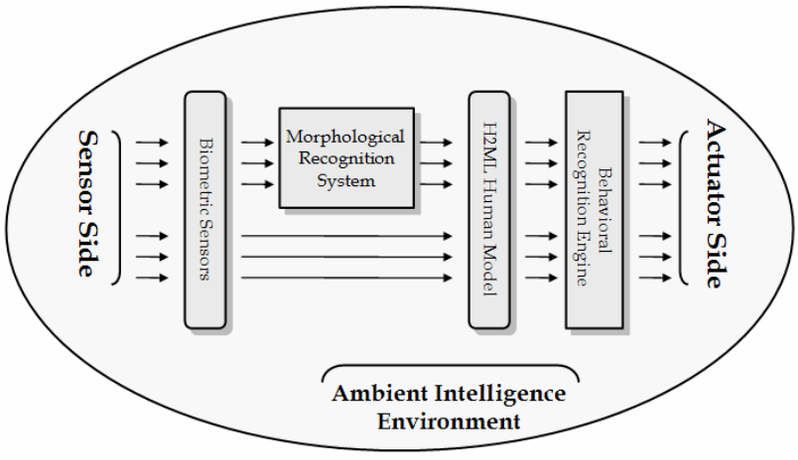

Figure 8. Ambient Intelligence Architecture

To design Ambient Intelligent Environments, many methodologies and techniques have to be merged together originating many approaches reported in recent literature (Basten & Geilen, 2003). We opt to a framework aimed to gather biometrical and environmental data, described in (Acampora et al., 2005) to test the effectiveness of face recognition systems to aid security and to recognize the emotional user status. This AmI system's architecture is organized in several sub-systems, as depicted in Figure 8, and it is based on the following

sensors and actuators: internal and external temperature sensors and internal temperature actuator, internal and external luminosity sensor and internal luminosity actuator, indoor presence sensor, a infrared camera to capture thermal images of user and a set of color cameras to capture information about gait and facial features. Firstly *Biometric Sensors* are used to gather user's biometrics (temperature, gait, position, facial expression, etc.) and part of this information is handled by *Morphological Recognition Subsystems* (*MRS*) able to organize it semantically. The resulting description, together with the remaining biometrics previously captured, are organized in a hierarchical structure based on XML technology in order to create a new markup language, called *H2ML* (*Human to Markup Language*) representing user status at a given time. Considering a sequence of H2ML descriptions, the *Behavioral Recognition Engine* (*BRE*), tries to recognize a particular user behaviour for which the system is able to provide suitable services. The available services are regulated by means of the *Service Regulation System* (*SRS*), an array of fuzzy controllers coded in FML (Acampora & Loia, 2004) aimed to achieve hardware transparency and to minimize the fuzzy inference time.
This architecture is able to distribute personalized services on the basis of physical and emotional user status captured from a set of biometric features and modelled by means of a mark-up language, based on XML. This approach is particularly suited to exploit biometric technologies to capture user's physical info gathered in a semantic representation describing a human in terms of morphological features.

4.1 Experimental Results

As one of the aims in experiments was to test the performance of the proposed method in a realistic operative environment, we decided to build a 3D face database from the face capture station used in the domotic system described above. The capture station featured two digital cameras with external electronic strobes shooting simultaneously with a shutter speed of 1/250 sec. while the subject was looking at a blinking led to reduce posing issues. More precisely, every face model in the gallery has been created deforming a pre-aligned prototype polygonal face mesh to closely fit a set of facial features extracted from front and side images of each individual enrolled in the system.
Indeed, for each enrolled subject a set of corresponding facial features extracted by a structured snake method from the two orthogonal views are correlated first and then used to guide the prototype mesh warping, performed through a Dirichlet Free Form Deformation. The two captured face images are aligned, combined and blended resulting in a color texture precisely fitting the reconstructed face mesh through the feature points previously extracted. The prototype face mesh used in the dataset has about 7K triangular facets, and even if it is possible to use mesh with higher level of detail we found this resolution to be adequate for face recognition. This is mainly due to the optimized tessellation which privileges key area such as eyes, nose and lips whereas a typical mesh produced by 3D scanner features almost evenly spaced vertices. Another remarkable advantage involved in the warp based mesh generation is the ability to reproduce a broad range of face variations through a rig based deformation system. This technique is commonly used in computer graphics for facial animation (Lee et al., 1995, Blanz & Vetter, 1999) and is easily applied to the prototype mesh linking the rig system to specific subsets of vertices on the face surface. Any facial expression could be mimicked opportunely combining the effect of the rig controlling lips, mouth shape, eye closing or opening, nose

tip or bridge, cheek shape, eyebrows shape, etc. The facial deformation model we used is based on (Lee et al., 1995) and the resulting expressions are anatomically correct.
We augmented the 3D dataset of each enrolled subject through the synthesis of fiften additional expressions selected to represent typical face shape deformation due to facial expressive muscles, each one included in the weighting mask. The fiften variations to the neutral face are grouped in three different classes: "good-mood", "normal-mood" and "bad-mood" emotional status (see Figure 9).
We acquired three set front-side pair of face images from 235 different persons in three subjective facial expression to represent "normal-mood", "good-mood" and "bad-mood" emotional status respectively (137 males and 98 females, age ranging from 19 to 65).

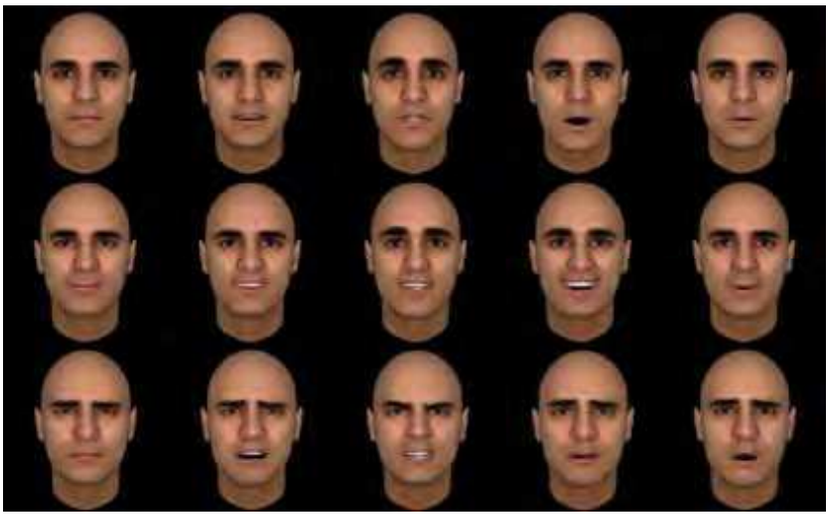

Figure 9. Facial Expressions grouped in normal-mood (first row), good-mood (second row), bad-mood (third row)

For the first group of experiments, we obtained a database of 235 3D face models in neutral pose (represented by "normal-mood" status) each one augmented with fiften expressive variations. Experimental results are generally good in terms of accuracy, showing a Recognition Rate of 100% using the expression weighting mask and flesh mask, the Gaussian function with σ=4.5 and k=50 and normal map sized 128 × 128 pixels. These results are generally better than those obtained by many 2D algorithms but a more meaningful comparison would require a face dataset featuring both 2D and 3D data. To this aim we experimented a PCA-based 2D face recognition algorithm [Moon and Phillips 1998, Martinez and Kak 2001] on the same subjects. We have trained the PCA-based recognition system with frontal face images acquired during several enrolment sessions (from 11 to 13 images for each subject), while the probe set is obtained from the same frontal images used to generate the 3D face mesh for the proposed method. This experiment has shown that our method produce better results than a typical PCA-based recognition algorithm on the same subjects. More precisely, PCA-based method reached a recognition rate of 88.39% on gray-scaled images sized to 200 × 256 pixels, proving that face dataset was really challenging.

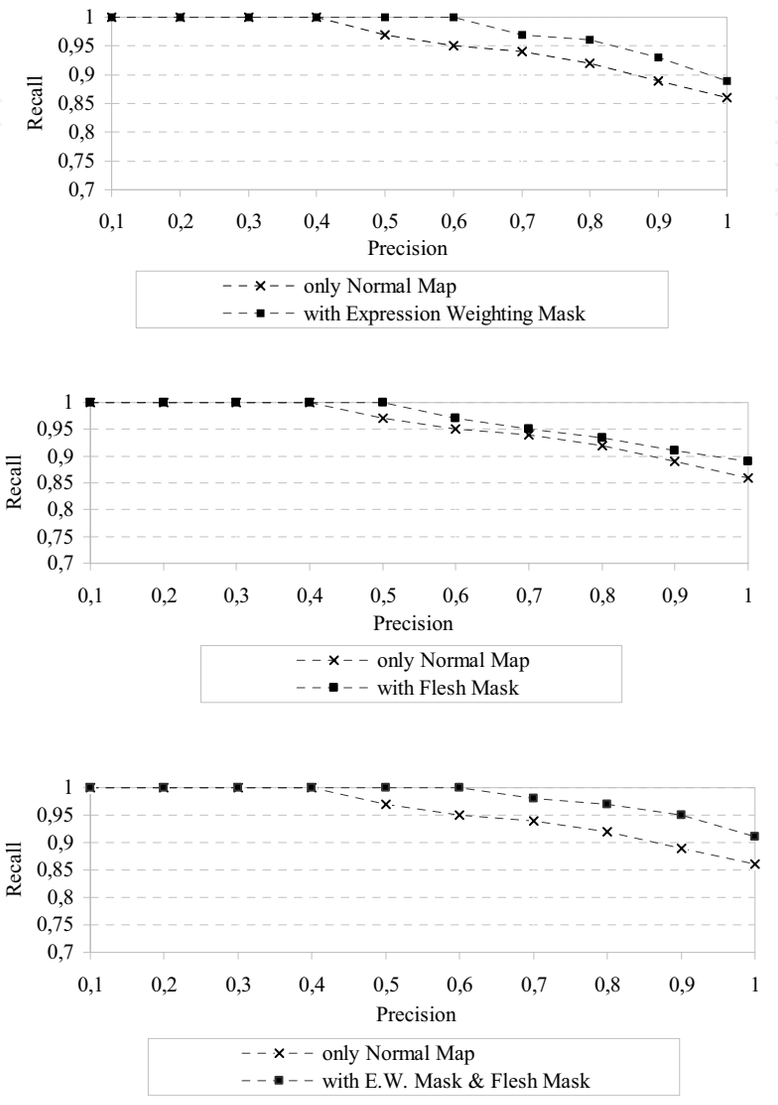

Figure 10. Precision/Recall Testing with and without Expression Weighting Mask and Flesh Mask to show efficacy respectively to (a) expression variations, (b) beard presence and (c) both

Figure 10 shows the precision/recall improvement provided by the expression weighting mask and flesh mask. The results showed in Figure 10-a were achieved comparing in one-to-many modality a query set with one expressive variations to an answer set composed by one neutral face plus ten expression variations and one face with beard. In Figure 10-b are shown the results of one-to-many comparison between subject with beard and an answer set

composed of one neutral face and ten expressive variations. Finally for the test reported in Figure 10-c the query was an expression variation or a face with beard, while the answer set could contain a neutral face plus ten associated expressive variations or a face with beard. The three charts clearly show the benefits involved with the use of both expressive and flesh mask, specially when combined together.

The second group of experiments has been conducted on FRGC dataset rel. 2/Experiment 3s (only shape considered) to test the method's performance with respect to Receiver Operating Characteristic (ROC) curve which plots the False Acceptance Rate (FAR) against Verification Rate (1 – False Rejection Rate or FRR) for various decision thresholds. The 4007 faces provided in the dataset have undergone a pre-processing stage to allow our method to work effectively. The typical workflow included: mesh alignment using the embedded info provided by FRGC dataset such as outer eye corners, nose tip, chin prominence; mesh subsampling to one fourth or original resolution; mesh cropping to eliminate unwanted detail (hair, neck, ears, etc.); normal map filtering by a 5 × 5 median filter to reduce capture noise and artifacts. Fig. 11 shows resulting ROC curves with typical ROC values at FAR = 0.001. The Equal Error Rate (EER) measured on all two galleries reaches 5.45% on the our gallery and 6.55% on FRGC dataset.

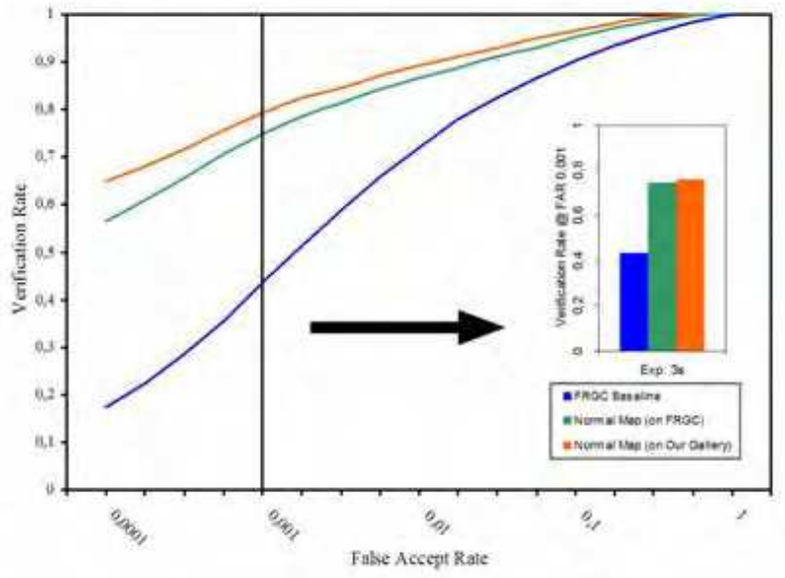

Figure 11. Comparison of ROC curves and Verification Rate at FAR=0.001

Finally, we have tested the method in order to evaluate statistically the behaviour of method to recognize the "emotional" status of the user. To this aim, we have performed a one-to-one comparison of a probe set of 3D face models representing real subjective mood status captured by camera (three facial expressions per person) with three gallery set of artificial mood status generated automatically by control rig based deformation system (fifteen facial expression per person grouped as shown in Figure 9). As shown in Table 1, the results are very interesting, because the mean recognition rate on "good-mood" status gallery is 100% while on "normal-mood" and "bad-mood" status galleries is 98.3% and 97.8% respectively

(probably, because of the propensity of the people to make similar facial expressions for "normal-mood" and "bad-mood" status).

Recognition Rate		
"normal-mood"	"good-mood"	"bad-mood"
98.3%	100%	97.8%

Table 1. The behaviour of method to recognize the "emotional" status of the user

5. Conclusion

We presented a 3D face recognition method applied to an Ambient Intelligence Environment. The proposed approach to acquisition and recognition proved to be suited to the applicative context thanks to high accuracy and recognition speed, effectively exploiting the advantages of face over other biometrics. As the acquisition system requires the user to look at a specific target to allow a valid face capture, we are working on a multi-angle stereoscopic camera arrangement, to make this critical task less annoying and more robust to a wide posing range.

This 3D face recognition method based on 3D geometry and color texture is aimed to improve robustness to presence/absence of beard and to expressive variations. It proved to be simple and fast and experiments conducted showed high average recognition rate and a measurable effectiveness of both flesh mask and expression weighting mask. Ongoing research will implement a true multi-modal version of the basic algorithm with a second recognition engine dedicated to the color info (texture) which could further enhance the discriminating power.

6. References

Aarts, E. & Marzano, S. (2003). The New Everyday: *Visions of Ambient Intelligence*, 010 Publishing, Rotterdam, The Netherlands

Acampora, G. & Loia, V. (2004). Fuzzy Control Interoperability for Adaptive Domotic Framework, *Proceedings of 2nd IEEE International Conference on Industrial Informatics*, (INDIN04), pp. 184-189, 24-26 June 2004, Berlin, Germany

Acampora, G.; Loia, V.; Nappi, M. & Ricciardi, S. (2005). Human-Based Models for Smart Devices in Ambient Intelligence, Proceedings of the IEEE International Symposium on *Industrial Electronics*. ISIE 2005. pp. 107- 112, June 20-23, 2005.

Basten, T. & Geilen, M. (2003). *Ambient Intelligence: Impact on Embedded System Design*, H. de Groot (Eds.), Kluwer Academic Pub., 2003

Beumier, C. & Acheroy, M. (2000). Automatic Face verification from 3D and grey level cues, *Proceeding of 11th Portuguese Conference on Pattern Recognition (RECPAD 2000)*, May 2000, Porto, Portugal.

Blanz, V. & Vetter, T. (1999). A morphable model for the synthesis of 3D faces, *Proceedings of SIGGRAPH 99*, Los Angeles, CA, ACM, pp. 187-194, Aug. 1999

Bronstein, A.M.; Bronstein, M.M. & Kimmel, R. (2003). Expression-invariant 3D face recognition, *Proceedings of Audio and Video-Based Person Authentication (AVBPA 2003)*, LCNS 2688, J. Kittler and M.S. Nixon, 62-70,2003.

Bowyer, K.W.; Chang, K. & Flynn P.A. (2004). Survey of 3D and Multi-Modal 3D+2D Face Recognition, *Proceeding of International Conference on Pattern Recognition*, ICPR, 2004

Chang, K.I.; Bowyer, K. & Flynn, P. (2003). Face Recognition Using 2D and 3D Facial Data, *Proceedings of the ACM Workshop on Multimodal User Authentication*, pp. 25-32, December 2003.

Chang, K.I.; Bowyer, K.W. & Flynn, P.J. (2005). Adaptive rigid multi-region selection for handling expression variation in 3D face recognition, *Proceedings of IEEE Workshop on Face Recognition Grand Challenge Experiments*, June 2005.

Enciso, R.; Li, J.; Fidaleo, D.A.; Kim, T-Y; Noh, J-Y & Neumann, U. (1999). Synthesis of 3D Faces, *Proceeding of International Workshop on Digital and Computational Video*, DCV'99, December 1999

Hester, C.; Srivastava, A. & Erlebacher, G. (2003) A novel technique for face recognition using range images, *Proceedings of Seventh Int'l Symposium on Signal Processing and Its Applications*, 2003.

Lee, Y.; D. Terzopoulos, D. & Waters, K. (1995). Realistic modeling for facial animation, *Proceedings of SIGGRAPH 95*, Los Angeles, CA, ACM, pp. 55-62, Aug. 1995

Maltoni, D.; Maio D., Jain A.K. & Prabhakar S. (2003). *Handbook of Fingerprint Recognition*, Springer, New York

Medioni,G. & Waupotitsch R. (2003). Face recognition and modeling in 3D. Prooceding of IEEE International Workshop on Analysis and Modeling of Faces and Gestures (AMFG 2003), pages 232-233, October 2003.

Pan, G.; Han, S.; Wu, Z. & Wang, Y. (2005). 3D face recognition using mapped depth images, *Proceedings of IEEE Workshop on Face Recognition Grand Challenge Experiments*, June 2005.

Papatheodorou, T. & Rueckert, D. (2004). Evaluation of Automatic 4D Face Recognition Using Surface and Texture Registration, *Proceedings of the Sixth IEEE International Conference on Automatic Face and Gesture Recognition*, pp. 321-326, May 2004, Seoul, Korea.

Perronnin, G. & Dugelay, J.L. (2003). An Introduction to biometrics and face recognition, *Proceedings of IMAGE 2003: Learning, Understanding, Information Retrieval, Medical*, Cagliari, Italy, June 2003

Tsalakanidou, F.; Tzovaras, D. & Strintzis, M. G. (2003). Use of depth and color eigenfaces for face recognition, *Pattern Recognition Letters*, vol. 24, No. 9-10, pp. 1427-1435, Jan-2003.

Xu, C.; Wang, Y.; Tan, t. & Quan, L. (2004). Automatic 3D face recognition combining global geometric features with local shape variation information, *Proceedings of Sixth International Conference on Automated Face and Gesture Recognition*, May 2004, pp. 308–313.

Wang, Y.; Chua, C. & Ho, Y. (2002). Facial feature detection and face recognition from 2D and 3D images, *Pattern Recognition Letters*, 23:1191-1202, 2002.

Face Recognition

Edited by Kresimir Delac and Mislav Grgic

ISBN 978-3-902613-03-5

Hard cover, 558 pages

Publisher I-Tech Education and Publishing

Published online 01, July, 2007

Published in print edition July, 2007

This book will serve as a handbook for students, researchers and practitioners in the area of automatic (computer) face recognition and inspire some future research ideas by identifying potential research directions. The book consists of 28 chapters, each focusing on a certain aspect of the problem. Within every chapter the reader will be given an overview of background information on the subject at hand and in many cases a description of the authors' original proposed solution. The chapters in this book are sorted alphabetically, according to the first author's surname. They should give the reader a general idea where the current research efforts are heading, both within the face recognition area itself and in interdisciplinary approaches.

InTech Europe
University Campus STeP Ri
Slavka Krautzeka 83/A
51000 Rijeka, Croatia
Phone: +385 (51) 770 447
Fax: +385 (51) 686 166
www.intechopen.com

InTech China
Unit 405, Office Block, Hotel Equatorial Shanghai
No.65, Yan An Road (West), Shanghai, 200040, China
中国上海市延安西路65号上海国际贵都大饭店办公楼405单元
Phone: +86-21-62489820
Fax: +86-21-62489821

IntechOpen